SUPPLEMENTARY INFORMATION

A. Calculation of excess mortality and morbidity attributable to influenza

Assessment of the mortality burden of influenza is not straightforward because severe complications triggered by influenza infection, such as bacterial pneumonia, are often diagnosed after the virus has been cleared [2, 24]. Many influenza-related deaths are therefore not coded as influenza but rather as underlying respiratory or chronic conditions. The traditional way to assess the mortality impact of influenza is to calculate excess mortality during influenza seasons, as the sum of deaths exceeding a baseline of expected deaths in the absence of influenza activity. Mortality from pneumonia and influenza (P&I) is considered a reliable indicator of the timing and relative severity of epidemics [2, 24].

Likewise, assessment of the morbidity burden of influenza is not straightforward because laboratory tests for influenza are rare; and in turn, non-specific outcomes such as hospital or physician visits for influenza-like-illness have to be studied. The influenza contribution to these outcomes can be estimated as the number of cases in excess above a seasonal baseline, where the seasonal baseline includes illnesses caused by co-circulating respiratory pathogens.

We describe below in detail the seasonal baseline model for P&I mortality; a very similar procedure was applied to morbidity data. To obtain a baseline for mortality in the absence of influenza, we applied a seasonal regression model adapted from the model

developed by the CDC in 1963 [28] and recently refined [8, 21]. Before applying the seasonal model, we detrended the time series of weekly P&I mortality rates in each country by fitting a spline smooth function of time to the mortality for the summer weeks (June-August). Then we divided the original time series by the spline trend, to obtain detrended series with constant level of summer mortality. We then applied a seasonal regression model to the detrended series in each country, $Y_{t,i}$, excluding values for December-April, following:

$$Y_{t,i} = a_i + b_i*cos(2\pi*t/52.1667) + c_i*\sin(2\pi*t/52.1667) + \varepsilon t_i,$$

where t is a running index for week of death, i is the country, and εt is the error term.

Weekly excess mortality rates in each country was calculated as the observed minus predicted mortality rate. *Seasonal excess mortality* was estimated as the sum of *weekly excess mortality* during December-April, after back-adjusting for the time trend. All terms included in our model were statistically significant ($p<0.0001$), but additional terms for time trends were not ($p>0.05$). We conducted a sensitivity analysis by using monthly instead of weekly data to estimate *seasonal excess mortality*.

Note that in the excess mortality or morbidity approach, the model baseline should be an accurate reflection of the level of mortality (morbidity) in the absence of influenza activity. The timing of influenza epidemic periods varies substantially from year to year, with a date of epidemic onset ranging between November and March. Hence with many years worth of data, observed mortality in the absence of influenza activity is available for all times of the year, ensuring that the baseline reflects true non-epidemic activity. In addition, in some rare seasons, influenza viral activity is so negligible that the entire winter can be used as non-epidemic period, allowing to check that the level of the

modelled baseline is accurate.

B. Sensitivity analyses

a) Model structure: distribution of the infectious period

In the simple SEIR model, an exponential distribution for the latent and infectious periods is implicitly assumed. That is, the probability that an infectious individual recovers (and progresses to the Protected class) is independent of the amount of time the individual has already spent in the infectious stage. Since the distribution of true latent and infectious periods tends to have narrower variance than exponential distributions, an improvement to this modeling assumption has been suggested via the use of stage-progression models, or the so-called linear chain trick [75]. In this approach, the latent and infectious periods are modeled as the progression in n_e latent sub-states and n_i infectious sub-states [76]. Overall, the resulting latent and infectious periods follow a gamma distribution with integer parameter n_e and n_i, respectively. When the rates of progression between sub-states is given by $n_e \kappa$ for the latent period and $n_i \gamma$ for the infectious period, the resulting gamma distribution has means $1/\kappa$ and $1/\gamma$ for the latent and infectious periods, respectively, and the corresponding variances are given by $1/(n_e \kappa^2)$ and $1/(n_i \gamma^2)$, respectively. This refinement over the traditional exponential distribution approach has proven important for modeling the dynamics of some infectious diseases, including influenza [37].

We carried out a sensitivity analysis to check that in the case of our seasonal influenza study, the magnitude of the bias in the estimated reproduction number (R_p)

was negligible. For this purpose, we have generated artificial epidemic curves using a realistic SEIR model with $n_e = n_i = 2$ as previously estimated for influenza [37], the natural history parameters from our main analysis ($1/\kappa = 1.9, 1/\gamma = 4.1$), and assuming a theoretical reproduction number $R_{th} = 1.3$ (equivalent to a theoretical $\beta_{th} = 0.317$, where $R_{th} = \beta_{th} / \gamma$), and a large population size ($N = 10^7$). We also added observational error in the simulated epidemic curves via the Poisson error structure described in the main analysis. Finally, we re-estimated the transmission parameter β from the artificial data by using the standard SEIR model with exponentially-distributed latent and infectious periods, to assess the bias in the estimated R_p.

The average scaled bias (ASB) for R_p is given by $\text{ASB} = \frac{1}{n} \sum_{i=1}^{n} (R_{p,i} - R_{th}) / R_{th}$, for n=1000 estimates obtained from simulated realizations with a known theoretical R_{th}. As shown in Figure S1, our results indicate that the bias incurred in our estimates of R_p rapidly vanishes with the amount of epidemic data used in the estimation. This bias is less than 10% when using 4 weeks of data or more, as in the main analysis.

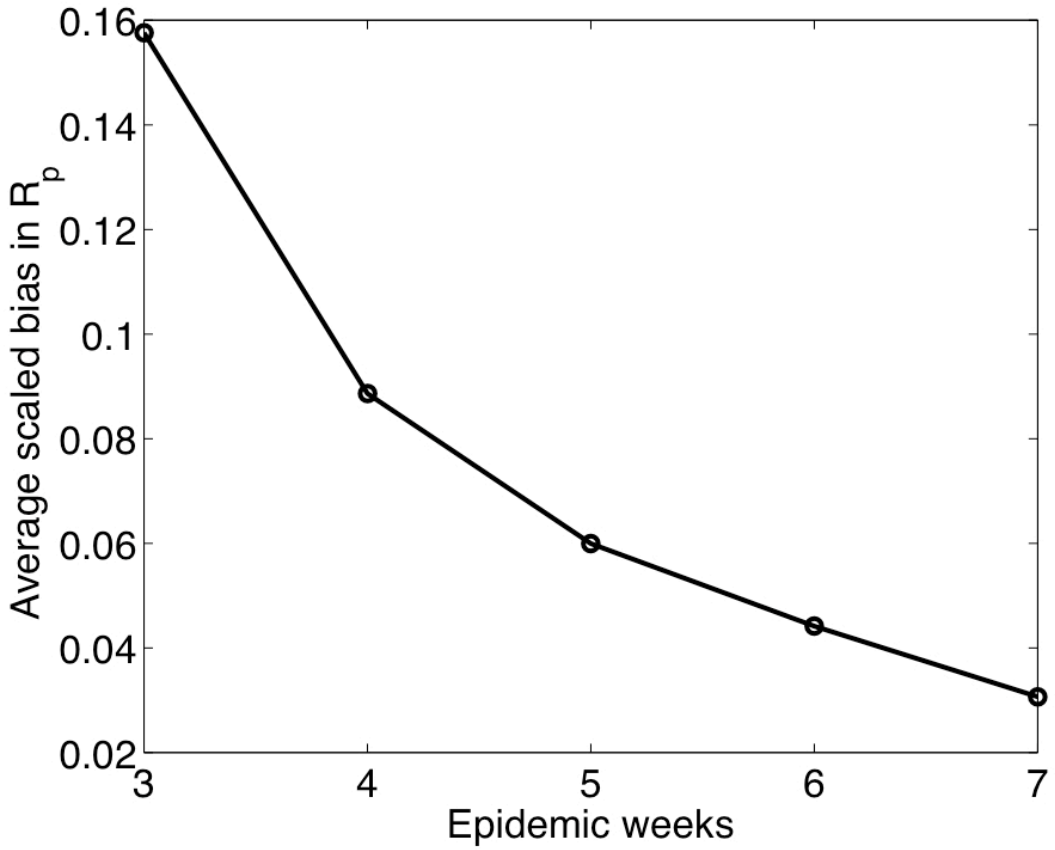

Figure S1 :Average scaled bias (ASB) in reproduction number estimate R_p when it is estimated with the simple SEIR model with exponentially-distributed latent and infectious periods, based on artificial influenza epidemic curves generated from a realistic SEIR epidemic model with $n_e = n_i = 2$ following [37]. The natural history parameters are those of the main analysis ($1/\kappa$=1.9,$1/\gamma$=4.1), and the theoretical reproduction number is set at R_{th}=1.3 ($\Leftrightarrow \beta_{th}$=0.317), and a large population size (N=10^7). For example, R_p is overestimated by less than 10% when using 4 epidemic weeks of data.

b) Model structure: distribution of errors

The larger the number of parameters estimated (2 in our case), the higher the variance of the parameter estimates. The worst case would be if the model parameters cannot be uniquely determined from the data, leading to unbounded variances of the estimates. In the main analysis, we have used a Poisson error structure to model measurement errors in the number of influenza deaths or cases. To test the robustness of our results to this assumption, we have also considered more extreme error structures, where the variance (σ^2) is several times greater than the mean (μ) of the observations (eg, Negative binomial or Gamma distributions). The resulting 95% confidence intervals do not change significantly when using extreme error structures, as shown in supplementary Table 1 for mortality data in the US. With gamma or negative binomial error structures, point estimates of the reproduction number R_p vary by less than 0.03 (3.3%). As expected, confidence intervals on Rp become larger when the modeled variance increases, but the difference is 0.24 (64.4%) at most in individual seasons estimates, and 0.05 (26.8%) on average over the 3-decade study period.

Supplementary table 1: Mean estimates of the reproduction number (R_p) for influenza seasons 1972-73 through 2001-02 using US mortality data and a negative binomial error structure where the variance (σ^2) is two, three, and four times larger than the mean (μ) observation. Results are essentially the same for a gamma distribution. Estimates using a Poisson error structure (as in the main analysis) are also shown for comparison.

	Poisson $\sigma^2 = \mu$		Neg. Binomial $(\sigma^2 = 2\mu)$		Neg. Binomial $(\sigma^2 = 3\mu)$		Neg. Binomial $(\sigma^2 = 4\mu)$	
	R_p	95% CI	R_p	95% CI	R_p	95% CI	R_p	95% CI
Mean, 1972-2002	**1.31**	**(1.21,1.41)**	**1.31**	**(1.21,1.41)**	**1.31**	**(1.21,1.41)**	**1.31**	**(1.21,1.41)**

c) Uncertainty of parameter estimates: profile likelihood

To check that parameters estimates were well-constrained and identifiable, we computed the likelihood ratio confidence bounds of the estimated parameters based on the equation $-2\log\left(\frac{L(\theta)}{L(\hat{\theta})}\right) \geq \chi^2_{\alpha,f}$ where $L(\theta)$ is the likelihood function for the unknown parameter vector $\theta = (\beta, E_0)$, $L(\hat{\theta})$ is the likelihood function evaluated at the estimated vector $\hat{\theta} = (\hat{\beta}, \hat{E}_0)$, and $\chi^2_{\alpha,f}$ is the chi-squared statistic with probability α and $f = 2$ degrees of freedom (number of parameters jointly estimated) [77]. We estimated numerically the likelihood function $L(\theta)$ for parameter values in a neighborhood of the best-fit parameter estimates $\hat{\theta} = (\hat{\beta}, \hat{E}_0)$ for all influenza seasons in the US, using mortality data. Our results indicate that our parameter estimates are indeed well constrained. Figure S2 below shows the contour plots for a cross-section of the likelihood function $-2\log\left(\frac{L(\theta)}{L(\hat{\theta})}\right)$ corresponding to 95% confidence intervals ($\chi^2_{0.95,2} = 5.99$) for the two estimated parameters (β, E_0) for four influenza seasons in the US. Note that β is directly related to the reproduction number R_p by the relation $R_p = \beta / \gamma$ (γ is the length of the infectious

period = 4.1 days)

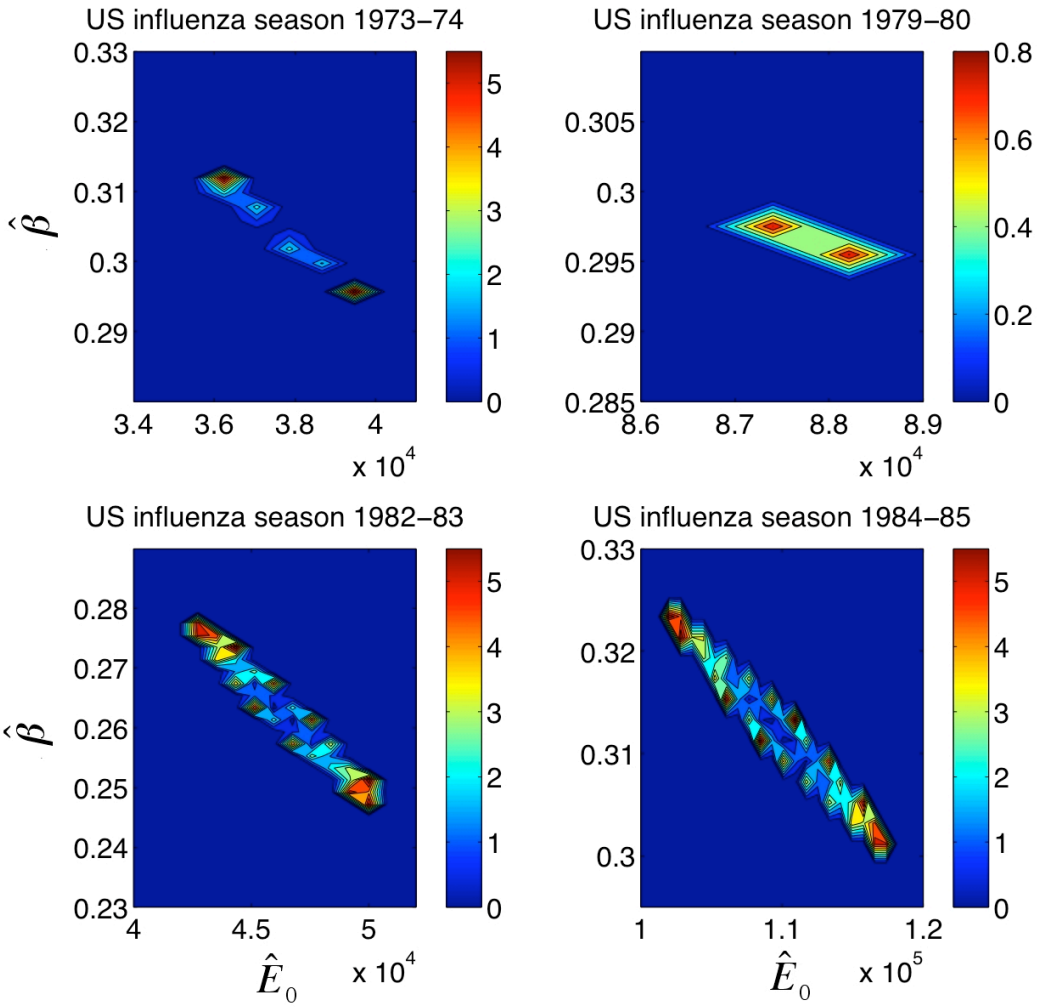

Figure S2: Contour plots of the likelihood ratio 95% confidence bounds for the two estimated parameters in four influenza seasons in the US, using mortality data.

Color bar: likelihood function $-2\log\left(\frac{L(\theta)}{L(\hat{\theta})}\right)$.

Estimating the probability of interrupting seasonal influenza transmission for different vaccination scenarios (Figure 7).

We first relied on the empirical cumulative distribution function of reproduction numbers estimated in this study, by combining estimates for the 3 countries. This gave P(Rp <=X), the probability that transmissibility (Rp) is below X for a randomly chosen influenza season. This probability is represented on the y-axis in figure 7. Next, for each value of transmissibility X, we can compute the herd immunity threshold (1-1/X), which is the proportion of the overall population that needs to be successfully immunized to interrupt transmission. Because we model vaccine strategies targeted at healthy population groups who respond well to the influenza vaccine (people aged 2-64 years, without chronic conditions), the target group size is only 72% of the overall population, using year 2000 population data. Assuming homogeneous mixing, a proportion (1-1/X)/0.72 of the healthy group needs to be successfully immunized to achieve herd immunity in the general population. Next, we can incorporate various vaccine efficacy estimates (VE, ranging from 60% to 99%) and calculate the minimal vaccine coverage in the healthy group necessary to interrupt transmission, following (1-1/X)/(0.72*VE) -- the x-axis in figure 7. Here, VE is the efficacy against secondary transmission of influenza, which is not precisely known for current influenza vaccines. By contrast, estimates of VE against infection and illness exist: influenza vaccination is estimated to prevent ~17-53% of laboratory-confirmed infections in the elderly [9], none in very young children under 2 years of age [69] and 70% in healthy adults and children [67, 68].